CrystEngComm

Accepted Manuscript

ROYAL SOCIETY OF CHEMISTRY

www.rsc.org/crystengcomm

Cocrystals of Telmisartan: Characterization, Structure elucidation, *In-vivo*, and Toxicity Studies

Renu Chadha[1*], Swati Bhandari[1], Jamshed Haneef[1], Sadhika Khullar[2] and Sanjay Mandal[2*]

[1]University Institute of Pharmaceutical Sciences, Panjab University, Chandigarh-160014, INDIA. E-mail: renukchadha@rediffmail.com; Tel: +91-9316015096
[2]Department of Chemical Sciences, Indian Institute of Science Education and Research, Mohali, Sector 81, Manauli PO, S.A.S. Nagar, Mohali (Punjab) 140306, INDIA. E-mail: sanjaymandal@iisermohali.ac.in; Tel:+91-9779932606

Abstract

The present study reports novel cocrystals of telmisartan (TEL) with saccharin and glutaric acid. Crystal engineering approaches such as solution crystallization, solid state grinding and slurry method have been utilized with the ultimate objective of improving the solubility of this BCS class II drug. The physical characterization revealed that the cocrystals are unique vis-a-vis thermal, spectroscopic and X-ray diffraction properties. Structural characterization showed that the cocrystals with saccharin and glutaric acid exist in Monoclinic $P2_1/c$ and Triclinic P-1 space groups, respectively. The improved solubility of telmisartan-saccharin (TEL-SAC) cocrystal (nine fold) and telmisartan-glutaric acid (two fold) in comparison to the free drug has been demonstrated in the solubility experiments in phosphate buffer pH 7.5. The TEL-SAC co-crystal remained stable in the aqueous medium for 6 hours as confirmed by PXRD. The AUC_{0-24} for TEL-SAC and TEL-GA was found to be 2 fold and 1.4 fold increased in bioavailability than pure TEL, respectively. The *in vivo* antihypertensive activity of TEL-SAC in DOCA salt induced hypertensive rats showed two fold improved efficacy, Acute toxicity studies revealed no signs of toxicity in rats even at doses of 2000 mg/Kg by body weight (BW). The new solid phase of telmisartan with saccharin represents a promising and a viable opportunity for the manufacture of a drug product with improved therapeutic outcome.

Introduction

Improvement of the physicochemical properties of APIs with solubility-limited bioavailability is of paramount importance in the pharmaceutical development of the drug molecules.[1,2] Pharmaceutical scientists have delved into exploring the scope of solid-state structural variations that can be obtained through salts, polymorphs and cocrystals of molecules assembled in a single lattice structure, in their

1

ever-increasing efforts to produce materials having improved properties notably, solubility, bioavailability and stability.[3,4]

A pharmaceutical cocrystal is defined as a multicomponent molecular complex comprising a solid API and a coformer (which is safe for human consumption), that interact through noncovalent interactions in a definite stoichiometric ratio [5-7] without compromising the structural integrity but improved solubility. Besides this, pharmaceutical cocrystals are considered as new chemical entities that impart many unique and useful properties to the parent compound and are suitable for intellectual property issues.[8]

In this context, cocrystallization of an antihypertensive drug, telmisartan, has been performed to improve its pharmaceutical properties. Telmisartan, an angiotensin-II antagonist is commercially available as Micardis® and Micardis plus®. The molecule is highly lipophilic (log P = 7.2) and has two pKa values of 4.7 (benzimidazole) and 6.7 (carboxyl).[9-11] The major issue that has limited the therapeutic efficacy of telmisartan is its poor solubility in physiological pH conditions resulting in poor and variable bioavailability (42%).[12] Therefore, many research groups have tried to improve its aqueous solubility and dissolution by use of self nanoemulsifying drug delivery system[13], amorphous formulation[14], nanoparticles[15], immediate release tablets[16] and solid dispersions.[17] However, crystal engineering approach has not been much explored except one article by Dinnebier et al. who have reported three crystal modifications (one solvate and two polymorphic forms A and B) that have been structurally characterized.[18] Telmisartan offers one acidic (hydrogen bond donor) and two basic (hydrogen bond acceptor) functionalities which represent suitable synthons (O-H…O, O-H….N, N-H….O, and N-H…N) for the formation of multicomponent crystals.[19-22] Along these lines, several acidic and basic salts of telmisartan with pharmaceutically acceptable agents have appeared in a patent with publication No. WO 2007/147889.[23] But the examples reporting the solubility, pharmacodynamics and acute toxicity studies of cocrystals are limited. One of the studies reporting a cocrystal of glutaric acid with sodium channel blocker showed significantly three times improvement *in* area under the curve during the *vivo* exposure to dogs as compared to the pure drug in a single dose experiment.[24] Beside this, cocrystallization of L-88355 with L-tartaric acid showed 20 fold increase in drug plasma levels of rhesus monkeys.[25] However, no reports on cocrystal of telmisartan have appeared till date. Thus, the present study is focused on the preparation of telmisartan-saccharin and telmisartan-glutaric acid cocrystals to enhance the solubility of telmisartan as well as obtain further insights into the structure of these engineered molecules. Saccharin and glutaric acid were selected as coformers due to their

2

pharmaceutical acceptability and have a propensity to enter into the supramolecular framework with a variety of molecules.

Experimental section

Materials: The anhydrous crystalline form of telmisartan was obtained as a gift sample from Unichem Piramal Healthcare, India. The investigated countermolecules, saccharin and glutaric acid were purchased from Himedia Labs, India. All other solvents and chemicals were of analytical grade.

Method: The telmisartan-saccharin cocrystal was prepared by three methods, solvent assisted grinding **TEL-SAC(G)**, slurry approach (**TEL-SAC)** and solution crystallization (**TEL-SAC(S))**. The telmisartan-glutaric acid cocrystal **(TEL-GA)** was prepared by refluxing a mixture of the two components.

(i) TEL-SAC(G) : Equimolar quantities of telmisartan 514.6 mg (1 mmole) and saccharin 183.2 mg (1 mmole) were ground in a pestle and mortar with addition of 5-6 drops of ethanol for one hour. The powder was dried and kept in air tight vials in a desiccator.

(ii) **TEL-SAC**: Equimolar quantities of telmisartan 257.3 mg (0.5 mmole) and saccharin 99 mg (0.5 mmole) were added to 3ml of ethanol in a 50 ml round bottom flask. The slurry was stirred and refluxed at 70 °C for 3 h. The solvent was evaporated at 60 °C under vacuum. The solid obtained was dried and stored in air tight vials in a desiccator.

(iii) **TEL-SAC(S):** 20 mg of TEL-SAC was dissolved in 2 ml of chloroform-isopropyl alcohol mixture (2:1 v/v) and allowed to evaporate slowly at room temperature. Crystals suitable for single-crystal X-ray diffraction analysis (size greater than 0.3x0.3x0.3 mm) were obtained in 2 days, filtered and dried under vacuum at 30 °C and stored in air tight vials.

(iv) (TEL-GA): Equimolar quantities of telmisartan (257.3 mg, 0.5 mmole) and glutaric acid (66.06 mg, 0.5 mmole) were added to 3ml of ethanol in a 50 ml round bottom flask. The slurry was stirred and refluxed at 30 °C for 24 h. The solvent was evaporated at 40 °C under vacuum. The solid obtained was dried and stored in airtight vials in desiccators.

Scanning Electron Microscopy

A Jeol JSM-6100 scanning electron microscope was used to obtain photomicrographs. Samples were mounted on a metal stub with an adhesive tape and coated under vacuum with gold.

Powder X-ray Diffraction (PXRD)

PXRD patterns of the investigated molecules were collected on X'Pert PRO diffractometer system (Panalytical, Netherlands) with a Cu Kα radiation (1.54060 Å). The tube voltage and current were set at 45 kV and 40 mA respectively. The divergence slit and anti-scattering slit settings were set at 0.48° for the diffraction experiment on the 10 mm sample size. Each sample was placed in an aluminium sample holder and measured by a continuous scan between 5° and 50° in 2θ with a step size of 0.017° and step time of 25 sec/step. The experimental XRPD patterns were refined using X'Pert High Score software.

Differential Scanning Calorimetry (DSC)

DSC analyses of the samples were performed on a DSC Q20 (TA Instruments, USA) which was calibrated for temperature and heat flow accuracy using indium (mp 156.6°C and ΔH of 25.45 J g^{-1}). The samples (3-5 mg) were placed in sealed non-hermetic aluminium pans and were scanned at a heating rate of 10 °C/min from 30 to 300 °C under a dry nitrogen atmosphere (flow rate 50 mL/min). The data were analysed using TA instruments Universal analysis 2000 software.

Thermogravimetric Analysis (TGA)

TGA was performed on a Mettler Toledo TGA/SDTA 851^e instrument. Approximately 5 mg sample was heated from 30 to 300 °C in open alumina pan at the rate of 10 °C/min under nitrogen purge at flow rate of 50 mL/min. The data were managed by STAR software (9.00).

Fourier Transform-Infra Red Spectroscopy (FT-IR*)*

A Spectrum RX I FT-IR spectrometer (Perkin Elmer, UK) was employed in the KBr diffuse-reflectance mode (sample concentration 2 mg in 20 mg of KBr) for collecting the IR spectra of samples. The spectra were measured over the range of 4000-400 cm^{-1}. Data were analyzed using Spectrum software.

Single crystal X-Ray diffraction

X-ray diffraction data sets were collected on a Bruker AXS Kappa APEX II diffractometer equipped with a CCD detector (with the crystal-to-detector distance fixed at 60 mm) using sealed-tube

4

monochromated Mo-Kα radiation (0.71073 Å) at room temperature (296 K). The crystal centering, unit cell determination, refinement of the cell parameters and data collection was controlled through the program APEX2.[26] The frames were integrated with the Bruker SAINT software package using a narrow-frame algorithm. Data were corrected for absorption effects using the multi-scan method (SADABS).[26] The structure was solved by direct methods using SHELXS-97 and refined against F^2 using SHELXL-97.[27] All calculations were performed using the SHELXTL V 11.0 suite of programs.[28] There were no residual peaks for all structures > 1e/A^3. All hydrogen atoms were placed in ideal positions and refined as riding atoms with individual isotropic displacement parameters. Crystallographic parameters and basic information pertaining to data collection and structure refinement for all compounds are summarized in Table 1. All figures were drawn using Mercury V 3.0[28] and hydrogen bonding parameters were generated using PLATON.[29] The final positional and thermal parameters of the non-hydrogen atoms for all structures are listed in the CIF files.

Crystal structure determination from PXRD

The crystal structure was determined from powder diffraction data using Reflex Plus module of Material Studio. The overall prediction process was carried out in four steps; indexing, Pawley fitting, structure solution and Rietveld refinement. In the indexing step, the crystal class and the approximate lattice parameters were derived from the peak positions in the experimental powder diffraction pattern using X-cell.[30] A table was generated from the results of X-cell that arranged the proposed unit cells according to their figure of merit. The unit cell with the highest figure of merit was selected and an empty unit cell was generated. The accurate lattice constants and the cell parameters were determined by Pawley fitting/refinement. The R_{wp} (weighted Rietveld parameter) value obtained after the refinement was used to establish the agreement between the calculated and the experimental powder patterns and hence confirm the accuracy of the crystal class and the lattice parameters. The space group that showed the highest figure of merit was selected and the pawley refinement was repeated with the selected space group to obtain another R_{wp}. The optimized structure of the drug molecule was imported into the refined unit cell and motion groups were defined. The structure was obtained using the Reflex Powder solve that involved Monte Carlo/simulated annealing procedure. 10 cycles of simulated annealing were selected with each cycle involving 2140100 number of steps. The similarity between the experimental and calculated diffraction patterns was confirmed by R_{wp} values. Further, Rietveld refinement of the structure solution was performed to obtain a final structure solution and a final R_{wp} value.

High Performance Liquid Chromatography

HPLC analysis was performed on a Waters Alliance system which includes a Waters 2695 separation module, a Waters 2996 Photodiode Array Detector and a 4.6 mm × 150 mm SunFire^{TM}C18, 5μm column)

Equilibrium solubility studies

Solubility of the TEL and TEL-SAC and TEL-GA were determined in phosphate buffer pH 7.5 at 25 °C. The solid samples were sieved through Gilson mesh sieve No.80 to obtain uniform particle size. An excess amount of solid phase (ca. 50 mg) was added to the 25 ml of buffer pre-equilibriated at 25 °C contained in a flask and the resulting slurry was shaken in a water bath shaker. Aliquots of the slurry were taken at various time intervals for a period of 6 hours to ensure that the solution has reached equilibrium.

Samples were filtered through 0.45 μm nylon filter and assayed for drug content by HPLC at 296 nm. The amount of drug dissolved in each time interval was calculated using the calibration curve which was prepared in phosphate buffer (pH 7.5). After a period of 24 hours, the residual solids were filtered, air dried and analyzed by DSC. The experiment was performed in triplicate and values expressed as mean± standard deviation.

Pharmacokinetics study

In order to determine blood levels of developed cocrystals, pharmacokinetic study was performed. The animals used for in the experiment were adult female wistar rats (weighing 180-200 g) kept under standard laboratory conditions. The animals were housed (4 rats per cage) with free access to standard laboratory diet.

Animals were divided in three groups of six each. Group I was given pure drug (TEL). Group II and Group III received cocrystals (TEL-SAC & TEL-GA, respectively). Single dose of all the preparations were suspended in 0.5% (w/v) sodium carboxymethyl cellulose (CMC) and administered by oral gavage. Each animal was treated with TEL dose equivalent to 1 mg/kg BW. The dose volume for all administration was maintained at 5 mL/kg BW. Serial blood samples were collected from retro-orbital venous plexus of rats at 0 (pre-dose), 0.5, 1, 2, 4, 6, 8, 10, 12, 18 and 24 hours into heparinised plastic tubes. The blood samples were then centrifuged at 10,000 rpm for 10 min. The plasma were separated and stored at -20º C until drug analysis carried out by RP-HPLC method [31]. Pharmacokinetic

parameters such as Cmax, AUC_{0-t} and relative bioavailability of pure drug and developed cocrystal were calculated by using non-compartmental analysis.

In vivo **pharmacodynamic activity**

Preparation and Administration of Doses

TEL and TEL-SAC were suspended in 0.5% (w/v) CMC (just before administration). CMC is used as a suspending agent as it is a relatively low cost, physiologically inert, safe and environmentally benign reagent and does not affect any of the vital organs of the body. [32] Single dose of both the preparations were administered by oral gavage. Each animal was treated with TEL dose equivalent to 1 mg/kg BW.

Antihypertensive activity evaluation

Evaluation of antihypertensive activity of TEL and its cocrystal were performed in DOCA-salt induced hypertensive rats.

4-5 weeks old female wistar rats (200-300g) were procured and maintained in the central animal house. Animals were housed (4 rats per cage) at a relative humidity of 65±2%, temperature of 25±2 °C with a 12-hour natural light/dark cycle. They were provided with standard pellet diet and water *ad libitum*. Experiments were performed as per guidelines of committee for the purpose of the CONTROL AND SUPERVISION ON EXPERIMENTS ON ANIMALS (CPCSEA). The experimental protocol was approved by Institutional Animal Ethics Committee (I.A.E. C.). After 1 week of adaptation to laboratory conditions, the animals were randomly assigned to 4 experimental groups each comprising of 6 animals (n=6).

Group I (Control group): These rats were vehicle treated. Cotton seed oil (0.1 ml/100 g) was injected subcutaneously twice a week for 6 weeks and 0.5% (w/v) CMC suspension was administered by oral gavage after 6 weeks.

Group II (DOCA +1% (w/v) NaCl - DOCA control group): In the second group, hypertension was induced in rats by subcutaneous injection of 15 mg/kg of DOCA dissolved in cotton seed oil, twice weekly for a 6 week period. Drinking water was replaced by 1% w/v sodium chloride solution (NaCl). The systolic blood pressure was recorded before and once weekly after the DOCA treatment. To establish the base line blood pressure, recordings were made at three separate occasions. After the

induction of hypertension (6 weeks) this group received a single oral dose therapy of CMC suspension daily for 6 days.

Group III (DOCA+1% (w/v) NaCl followed by TEL): Similar to group II, this group received DOCA and 1% (w/v) NaCl solution for 6 weeks. After the induction of hypertension (6 weeks) this group received a single oral dose therapy of 1 mg/kg of TEL in 0.5% (w/v) CMC suspension daily for 6 days.

Group IV (DOCA+1% (w/v) NaCl followed by TEL-SAC cocrystal): Similar to group II, third group received DOCA and 1% (w/v) NaCl solution for 6 weeks followed by a single oral dose therapy of TEL-SAC cocrystal equivalent to 1 mg/kg TEL for 6 days.

Changes in arterial blood pressure of all the groups were recorded after 24 hours of dose administration every day for 7 days to evaluate the antihypertensive efficacy of the new telmisartan cocrystal in comparison to the groups I (control), II and III.

Blood pressure recording in rats

The arterial blood pressure of each rat was measured at weekly intervals for 6 weeks, by the tail cuff method. The systolic blood pressure of each rat was measured at weekly intervals for 6 weeks. The rat tail was heated with 200 W bulb heat lamp for 3-5 min and mean arterial blood pressure (MABP) was recorded using non-invasive blood pressure measurement technique (NIBP- Biopac-MP 100, USA). At least 3 separate indirect pressures were averaged for each animal. The animals having MABP $\geq$ 180 mmHg were considered as a hypertensive.[33]

Statistical analysis

Data was expressed as mean (M) ± standard deviation (SD). One way analysis of variance (ANOVA) was used for each parameter, followed by Tukey's test. P<0.001 is considered statistically significant.

Acute Oral Toxicity

Preparation of doses for acute oral toxicity

TEL and TEL-SAC were dispersed in 0.5% carboxymethylcellulose suspension at a concentration of 1.000 g/ml. Suitable volumes of TEL and TEL-SAC were administered to achieve the required doses. The doses were prepared at the same time, one hour before administration.

Selection of animals and housing

8

Healthy young adult nulliparous and nonpregnant female Wistar rats, weighing 100-120 g (10-12 weeks old, at the start of the experiment), were procured from Central Animal House of Panjab University, Chandigarh, India. The present study was approved by Institutional Animal Ethics Committee of Panjab University, Chandigarh, India. The animals were randomly selected and kept in their cages for 7 days prior to dosing to allow for their acclimatization to the laboratory conditions. The animals were housed one animal per cage, at 22°C (±3°C) temperature and relative humidity of 45% (±5) with natural day/night cycles (approximately 12hr dark/light) and supplied with drinking water, *ad libitum* and standard rat chow (20 g/animal/day). Clean paddy husk bedding was provided to the animals which was changed every third day. The group of animals to which telmisartan was administered, were coded as TEL-1 to 5 while for telmisartan-saccharin co-crystal group the animals were coded as TEL-SAC-1 to 5.

Main test

As no information is available to make a preliminary estimate of the LD50 for telmisartan and its combination with saccharin (especially because of variations in reported LD50 of telmisartan from 980 to >2000 mg/Kg BW [34], hence the dosing was started at 175 mg/Kg BW in concordance with the guidance of OECD TG 425 [35] to produce the best results. The volume of TEL/TEL-SAC administered at any given time was not more than 2 ml/animal/30 minutes. All animals were fasted overnight prior to dose administration. Food was withheld further for a period of 2-3 hours after completing the dose administration. The animals were dosed one at a time. Using the default progression factor (aot425 software), the calculated initial dose TEL and TEL-SAC was thus 175 mg/Kg BW followed by 550, 1750 and 5000 mg/Kg BW. All the doses were calculated based on telmisartan content in combinations.

Observations

Animals were observed individually during the first 30 minutes after completing the dosing and periodically thereafter during the first 24 hours (special attention was paid to the animals during the first 4 hours), and daily thereafter, for a total of 14 days. All observations were systematically recorded with individual records being maintained for each animal. Observations included change in skin, fur, eyes and mucous membranes and behaviour patterns. Attention was given for observations of tremors, convulsions, salivation, diarrhoea, lethargy, sleep and coma. Individual weights of animals were recorded before the administration of drug on 1st day of the study and thereafter on the 7th and 14th day

of the experiment. Changes in weights of individual animals were calculated and compared with that of the control animals.

Pathological examination of various organs

To examine the pathological changes, the exposed rats were anesthetized, post the 14 day observation period, by pentobarbital injection, i.p. and autopsied. The organs such as stomach, liver and kidney were stripped out and fixed immediately in 10% formalin. Organ samples were embedded in paraffin blocks, sliced, fixed on glass slide, stained (H-E staining), observed and photographed using optical microscope.

Statistical analysis

Change in BW was expressed as mean (M) ± standard deviation (SD) and statistical significant differences were evaluated using t-test. LD50 was determined using the official statistical program (aot425, Version: 1.0).

Result and discussion

Co-crystals of telmisartan were prepared with two coformers, saccharin and glutaric acid**.** Their structures are given in Scheme 1.

Three separate methods were used for the cocrystallization of telmisartan with saccharin (Scheme 2) that resulted in amorphous, crystalline and solvated forms of cocrystal. Solvent assisted grinding of telmisartan and saccharin resulted in an amorphous microparticulate powder. The cocrystal obtained by slurry method appeared to be crystalline in nature but not suitable for single crystal analysis. Thus, solution crystallization method was utilized, that resulted to sufficiently large sized crystals to be studied by single crystal X-ray crystallography. Various solution crystallization experiments performed in variety of solvents resulted in precipitation of individual component. Use of a mixture of solvents could not produce convincing results except one experiment in which chloroform and isopropyl alcohol were used. Preliminary characterization of the form obtained from recrystallization by optical microscopy showed tabular crystals in contrary to the fine needle shaped crystals of telmisartan (Figure 1). The structure of TEL-SAC(S) was determined by single crystal X-ray diffraction.

Traditional solution-based experiments did not yield telmisartan-glutaric acid co-crystal. However, refluxing a physical mixture of telmisartan and glutaric acid with a small amount of solvent yielded

fruitful results. DSC and PXRD patterns of the products indicated that it was indeed a unique solid form. The structure of this co-crystal was determined from the PXRD data.

All the newly formed multi-component forms were further characterized using various analytical techniques.

Powder X-ray diffraction (PXRD)

The PXRD pattern of a crystalline sample is considered as the fingerprint of its crystal structure. Every new crystalline material exhibits unique peaks indicative of reflections from specific atomic planes.[36]

The PXRD patterns for TEL, SAC, TEL-SAC(G), TEL-SAC and TEL-SAC (S) are summarized in figure 2 A and 2B. Characteristic reflections at 2θ values of 6.8, 14.3, 15.1, 19.1, 22.4 and 23.9˚ were observed in case of telmisartan. Appearance of an amorphous halo pattern in the PXRD of TEL-SAC (G) indicated its amorphous nature. TEL-SAC prepared by slurry technique showed unique crystalline peaks at 2θ values of 5.4, 8.4, 11.3, 12.0, 25.3, 25.8 and 30.16°. Similarly, TEL-SAC(S) prepared by solution crystallization exhibits distinguishable reflections different from those of the constituents and characteristic diffraction peaks of telmisartan were also absent in case of TEL-SAC(S). The PXRD pattern of TEL-GA showed new peaks at 2θ values of 7.1°, 7.8°, 11.6°, 13.9°, 19.8° and 23.0° which were absent in both the drug and the co-former (figure 3). Besides this, peaks at positions 16.9°, 18.4°, 23.9°, 25.1°, 29.3°,31.2°, 32.4° and 38.1° present in TEL were absent in case of TEL-GA.

Differential Scanning Calorimetry (DSC) and Thermogravimetric Analysis (TGA)

The DSC scan of telmisartan (Form A) showed a single melting endothermic event at 268.9 °C . In the DSC scan of TEL-SAC(G) (Figure 4), an exotherm peak at 150 °C is ascribed to a recrystallization event suggesting the conversion of this amorphous form to crystalline state that finally melts at 219.4 °C (enthalpy of fusion 60.53 J/g). This temperature of melting is different from the melting points of drug (268.9 °C) and the coformer, saccharin (229.8 °C).

Two endothermic events appeared in the DSC scan of TEL-SAC(S) obtained from solution crystallization from chloroform-isopropyl alcohol mixture. The first endotherm at 202 °C is accompanied by mass loss in TGA indicating it to be a solvate. Stoichiometric calculations for chloroform as well as isopropyl alcohol suggest the existence of chloroform as entrapped solvent which was confirmed by SCXRD. TEL-SAC(S) finally melts at 219.8 °C. This shows that TEL-SAC(S) is a chloroform solvate of telmisartan-saccharin co-crystal. However, TEL-SAC obtained from the slurry

11

method depicted a single thermal event at 219.2 °C without any weight loss in the TGA negating the presence of any solvation or transition. It is interesting to mention that the amorphous and the solvated forms are transformed to the form similar to the phase obtained from slurry technique (219.2 - 219.8 °C).

The DSC scan of TEL-GA showed two endothermic peaks at 160 °C and 236 °C (figure 5A) with a corresponding mass loss of 18.17% in the TGA scan (figure 5 B). This showed that melting of the cocrystal was simultaneously associated with loss and decomposition of glutaric acid. The weight loss in TGA correlated well with theoretical weight loss of 20.39 % corresponding to a single molecule of glutaric acid suggesting a stoichiometry of 1:1 between TEL and GA.

Both PXRD and DSC indicated new phases in samples TEL-SAC (G), TEL-SAC and TEL-SAC(S) and TEL-GA.

The new phases could either be a salt or a co-crystal due to a pK_a difference of 2.4 and 1.8 between telmisartan and the co-formers, saccharin and glutaric acid respectively. Now, as the cocrystal formation with saccharin requires an API of sufficiently low basicity, there are chances of formation of a co-crystal with saccharin, which was confirmed by single crystal X-ray diffraction (SCXRD) and fourier transform infrared spectroscopy (FT-IR).

Fourier Transform-Infra Red Spectroscopy

In FT-IR spectroscopy, the vibrational changes serve as probes of intermolecular interactions in solid materials. The FT-IR spectrum for telmisartan (figure 6) showed peaks at 3473, 3058 and 1695 cm^{-1}, corresponding to the carboxylic –OH stretch, aromatic –CH stretch and -C=O stretch respectively. A decrease in –C=O stretch frequency of telmisartan from 1695 cm^{-1} to 1623 cm^{-1} in TEL-SAC(G), 1658 cm^{-1} in TEL-SAC and 1661 cm^{-1} in TEL-SAC(S) implies that the –C=O group is participating in some kind of interaction.

Similarly, in case TEL-GA, a shift in -C=O stretch from 1695 cm^{-1} to 1710 cm^{-1} indicates the presence of interactions involving the carbonyl group (figure 7). The absence of peaks corresponding to NH_3^+ molecule in the region of 3100-2500 cm^{-1} and -C=O stretch corresponding to the carboxylate salts from 1750-1700 cm^{-1} shows that in TEL-SAC and TEL-GA, both the drug and the coformer are present in the neutral state. This suggests the formation of cocrystals.

Single crystal X-ray diffraction (SCXRD)

TEL-SAC(S) crystallizes in the Monoclinic space group $P2_1/c$ with the asymmetric unit consisting of two independent molecules of telmisartan, saccharin and chloroform in the ratio of 1:1:1 (Figure 8). There is no proton transfer involved among the telmisartan and the saccharin molecules while chloroform molecules are entrapped in the crystal lattice. Thus, TEL-SAC is a co-crystal chloroform solvate. The crystal structure of TEL-SAC consists of zigzag chains of telmisartan molecules formed through intermolecular hydrogen bonded contacts involving nitrogen atom of the central benzimidazole fragment of telmisartan and the –OH group of another telmisartan molecule, i.e., N..H-O contacts (N7…H3A O3 (N/O 2.661 Å, N/H 1.84 Å, N-H/O 167°). The hydrogen bond attached to the nitrogen atom of terminal benzimidazole fragment of one telmisartan molecule is further H-bonded to another saccharin molecule via N1H6….N9 contact (N/O 2.661 Å, N/H 1.84 Å, N-H/O 167 °) (Figure 9A). Chloroform molecules are entrapped within the voids of the crystal lattice with no bonding with the neighbouring molecules. The packing diagram of the cocrystal solvate is shown in Figure 9B. The structural information and hydrogen bond geometries are given in Table 1 and Table 2, respectively. The experimental and the simulated PXRD patterns of the new phase TEL-SAC(S) are compared in Figure 2C. The resemblance of the two patterns validates the method of preparation and indicates the purity of the new phase.

Crystal structure determination by PXRD

Crystal structure of TEL-GA was determined from powder X-ray diffraction as discussed in the experimental section. Rwp value of 7.74 was obtained during the crystal structure determination of TEL-GA (Figure 10). TEL-GA crystallizes in the Triclinic crystal system with space group *P-1*. The unit cell consists of two telmisartan and two glutaric acid molecules (Figure 11A). The crystallographic parameters are given in Table 3. As shown in Figure 11B, TEL-GA cocrystal forms a heterosynthon (H—O… O) involving the carbonyl group of TEL and hydroxyl group of GA molecule. Similarly, another heterosynthon is formed by the H-bonding between hydroxyl group of TEL and carbonyl group of GA molecule.

Desolvation and heat mediated phase transformation of the cocrystal solvate (TEL-SAC(S))

In order to gain insight into the heat mediated phase transformation of the TEL-SAC(S), desolvation experiments were conducted by heating 200 mg of the cocrystal solvate at 140 °C in a vacuum oven

(130 mm Hg) for 5 hours. The resulting desolvated material was analyzed by PXRD and DSC to study the structural changes which occurred owing to the desolvation process. PXRD patterns (figure 2B) of the desolvated form showed a decrease in degree of crystallinity. Thus, removal of the solvent molecules from the crystal lattice resulted in a structural rearrangement with partial loss of crystallinity. However, the DSC results (figure 4B) showed an exotherm at 160 °C succeeded by an endotherm at 220 °C. This indicates the heat induced transition of partially crystalline desolvated cocrystal into crystalline form that finally melts at 220 °C. Moreover, no change was observed in FT-IR patterns of the desolvated form of the cocrystal (figure 6B) indicating the existence of the co-crystal even after the desolvation process.

Equilibrium solubility studies

Out of the cocrystals prepared by different methods, the one formed by slurry method was subjected to equilibrium solubility studies because desolvation and the heat mediated phase transformation of TEL-SAC(S) has led to this form (TEL-SAC) only. The solubility profile of TEL-SAC and TEL in phosphate buffer pH 7.5 at 25 °C revealed that the saturation solubility of the cocrystal (63μg/ml) was achieved in less than 20 min. The cocrystal showed nine fold increase in solubility of TEL which was sustained even after 6 hours of the study. The pH of the solutions during the solubility experiment remained constant. The residual solids after 6 and 24 hours of the solubility study were analysed by DSC (Figure 12) to investigate any change in the drug and the cocrystal. The studies revealed that both the drug and the cocrystal were intact upto 6 hours. After 24 hours, the DSC pattern in case of TEL-SAC cocrystal revealed two endotherms at 96 °C and 151 °C (accompanied by a weight loss at 96 °C) followed by the melting endotherm of TEL (264.5 °C). This suggests the formation of a hydrate which is desolvated at 96 °C. Absence of a mass loss in TGA at 151 °C confirmed the presence of a new form of telmisartan which is different from the existing forms A, B and C. This indicates that the cocrystal releases the free drug and this phase transformation generates a new hydrated form of the drug. This new form is further being investigated in our laboratory. TEL-GA showed a two-fold enhancement (14.4 μg/mL) in drug release in comparison to Form A of telmisartan within 15 minutes. However, the co-crystal was not stable up to 6 hours evident from the DSC scan of the residue after solubility analysis (Figure 13). The solubility of developed cocrystals was significantly higher than TEL ($P < 0.001$) as listed in Table 4.

The superior physicochemical properties of the new engineered drug molecule (TEL-SAC) inspired its further development and thus in-vivo studies as well as toxicity studies were performed.

Pharmacokinetics study

Telmisartan plasma concentration was assessed by sensitive RP-HPLC method. The pharmacokinetic parameter of pure drug TEL, TEL-SAC and TEL-GA were calculated using trapezoidal rule and are shown in Table 5 and Figure 14. The data show that AUC_{0-24} for TEL-SAC and TEL-GA was found to be 2 fold and 1.4 fold increased in bioavailability than TEL, respectively. The Cmax of TEL-SAC was found to be 1.318 µg/mL as compared to TEL (0.794 µg/mL). The Cmax of TEL-GA was found to be 0.998 µg/mL, slightly increased as compared to TEL. The higher plasma concentration of TEL-SAC than TEL-GA and TEL justifies its better water solubility and enhanced in vivo absorption of the drug.

In vivo pharmacodynamic studies

Antihypertensive activity evaluation

The blood pressure of the control rats (group I) was between 120-130 mm Hg which remained constant throughout the study period. However, the DOCA induced rats (group II, III and IV) showed an elevated blood pressure levels after 2 week of treatment and a mild but significant hypertension. A marked increase in blood pressure levels were observed which reached between 180 and 210 mm Hg after 6 weeks.

After the oral administration of CMC to groups I and II, changes in the systolic blood pressure were recorded and expressed as percentage decrease in the systolic blood pressure. No noteworthy change in the blood pressure levels of rats during the experimental period was observed (figure 14).

The systolic blood pressure of the control rats (group I) was between 120-130 mm Hg which remained constant throughout the study period. However, the DOCA induced rats (group II, III, IV, V and VI) showed elevated blood pressure levels after 2 week of treatment and a mild but significant hypertension. A marked increase in blood pressure levels was observed which reached between 180 and 210 mm Hg after 6 weeks.

After the oral administration of CMC to groups I and II, changes in the systolic blood pressure were recorded and expressed as percentage decrease in the systolic blood pressure. No noteworthy change in the blood pressure levels of rats during the experimental period was observed.

After this, treatment of groups III and IV with TEL form A, TEL-SAC respectively once daily for a period of 6 days led to significant attenuation of the elevated systolic blood pressure levels of these

DOCA salt induced hypertensive rats in comparison to the groups I and II (P< 0.001) (Figure 15). Following the dose treatment, the maximum decrease of systolic blood pressure was 25.8 ±1.2% in form A and 33.2±1.4% in TEL-SAC. The experimental data was statistically analysed by ANOVA and significant decrease in the arterial blood pressure due to TEL-SAC as compared to the control, DOCA control and the form A was observed (P ≤ 0.001) at all points.

The enhanced antihypertensive activity of the TEL-SAC cocrystal is attributed to the increased solubility of the drug when hydrogen bonded to the highly water soluble saccharin which led to its elevated absorption. Conclusively, the pharmacodynamic activity of the prepared cocrystal demonstrated the role of pharmaceutical cocrystals in bioavailability enhancement of poorly water soluble telmisartan.

Now, improved solubility and pharmacodynamic activity inspired us to evaluate the toxicological profile of the prepared cocrystal which is important in the design of formulation and could capture the potential of this novel cocrystal.

Acute toxicity studies

The toxicity studies were performed to confirm the safety of the developed TEL-SAC cocrystal against the pure TEL.

<u>Body weight</u>

No significant changes were observed in BW at the determined LD_{50} values (Table 6 & Table 7) for both TEL and TEL-SAC.

<u>Wellness parameters</u>

Skin, fur, eyes, mucous membrane, behavioural pattern, salivation and sleep of the treated as well as the control animals were found to be normal. No signs of toxicity or death was observed in all the animals treated with telmisartan and cocrystal at doses equivalent to 630 mg of TEL /Kg BW and 2000mg /Kg BW for TEL and TEL-SAC. The LD50 of TEL and TEL-SAC was thus found to be >2000 mg/Kg BW as per the aot425 software.

<u>Histopathological findings</u>

The acute and chronic toxicity studies of telmisartan by oral and intravenous routes have been reported earlier. However, histopathology findings are missing in case of acute toxicity studies. The major side

effects which have been reported during the chronic toxicity experiments with TEL include ulcers and erosions of the mucosa of the glandular stomach, hyperplasia of the epitheliod cells of the juxtraglomerular apparatus of kidney and patch-like cytoplasmic basophilia of the centrilobular hepatocytes.

Hence, the animals were observed for histopathological changes in the sections of stomach, liver and kidney. All the sections of stomach, kidney and liver were grossly normal at the tested dose of TEL equivalent to 2000 mg/kg BW (figure 16).

Thus, the histopathological findings support the LD50 values (>2000 mg equivalent to telmisartan/KG BW) of the cocrystal calculated using aot425 software.

Conclusions

A successful application of crystal engineering approach to achieve enhanced solubility of this poorly water soluble antihypertensive drug has been demonstrated by the cocrystal of telmisartan with saccharin. TEL-SAC was found to be relatively more soluble and showed significant increase in oral bioavailability in rat plasma. Improved efficacy in terms of percentage decrease in arterial blood pressure in DOCA induced hypertensive rats was also observed. TEL-SAC was found to be equally safe as TEL which is exhibited by the LD50 values. The histopathological evidence gained through the examination of stomach, liver and kidney also confirm the safety of the cocrystal. Conclusively, TEL-SAC shows immense potential in terms of improved antihypertensive efficacy and safety that makes it a suitable candidate for an optimal formulation.

Electronic Supplementary Information (ESI) available: Crystallographic data of the structure TEL-SAC(S) in CIF format (CCDC number 989764)

References

(1) C. B. Aakeröy, D.J. Salmon, *CrystEngComm.* 2005, **7**, 439 – 448.

(2) P. Vishweshwar, J. A. McMahon, J. A. Bis, M. J. Zaworotko, *J. Pharm. Sci.* 2006, **95**, 499 – 516.

(3) N. Shan and M. J. Zaworotko, *DrugDiscoveryToday*. 2008, **13**, 440 – 446.

(4) G. R. Desiraju, Angew. *Chem. Int. Ed*., 1995, **34**, 2311 – 2327.

(5) G. P. Stahly, *Cryst.Growth Des*. 2009, **9**, 4212 – 4229.

(6) W. Jones, W.D.S Motherwell, A.V. Trask, *MRS Bull*, 2006, **31**, 875 – 879.

(7) US Food and Drug administration approved GRAS list. EAFUS: A food additive database. http://www.fda.gov/food/foodingredientspackaging/foodadditives/foodadditivelistings/ucm091048.htm. (Assessed on 16-06-2012)

(8) A.V. Trask, *Mol. Pharm.* 2007, **4(3)**, 301 – 309.

 (9) E. Cagigal, L. Gonza´lez, R.M. Alonso, R.M. Jime´nez, *J. Pharm. Biomed. Anal.* 2001, **26**, 477–486.

 (10) U.J. Ries, G. Mihm, B. Narr, K.M. Hasselbach, H. Wittneben, M. Entzeroth, J.C. Van Meel, W. Wienen, *J.Med.Chem.* 1993, **36,** 4040 – 4051.

 (11) E.C. Demiralay, B. Cubuk, S. A. Ozkan, G. Alsancak, *J. Pharm. Biomed. Anal.* 2010, **53**, 475 – 482.

 (12) J. Stangier, S. Capf, W.Roth, *J.Int.Medic.Res.* 2000, **28**, 149 –167.

(13) J. Patel, G. Kevin, A. Patel, M. Raval, N. Sheth, *Int.J.Pharm.Educ.* 2011, **1**, 112 – 118.

(14) P. Koilkonda, A.R. Lekkala, C.M.K. Golla, S.R. Ganji, R.B. Konda, US Patent, 0111417 A1. 2006

(15) Y. Zhang, T. Jiang , Q. Zhang , S. Wang , *Eur. J. Pharm. Biopharm*. 2010, **76(1)**, 17 – 23.

(16) V. Sekar, V.R. Chellan, *Chem. Pharm. Bull*. 2008, **56(4)**, 575 – 577.

 (17) P.H.L.Tran, H.T.T. Tran, B.J. Lee, *J.Control.Rel*. 2008, **129**, 59 – 65.

(18) R.E. Dinnebier, P.Sieger, H. Nar, K.Shankland, W.I.F David, *J. Pharm. Sci.* 2000, **89 (11)**, 1465 – 1479.

(19) B. R. Bhogala, S. Basavoju, A. Nangia, *CrystEngComm.* 2005, **7**, 551 – 562.

(20) J. A. Bis, M. J. Zaworotko, *Cryst. Growth Des.* 2005, **5(3)**, 1169 – 1179.

(21) B. R. Bhogala, A. Nangia, *Cryst. Growth Des.* 2003, **3**, 547 – 554.

(22) C. B. Aakero¨y, A. M. Beatty, B. A., M. Helfrich, *Cryst. Growth Des.* 2003, **3**, 159 – 165.

(23) S. Zupancic, M. Smrkolj, T. Stropnik, M. Vrbinc, R. Osolnik, G. Sedmak, World Patent WO 147889, 2007.

(24) D.P. McNamara, S.L. Childs, J. Giordano, A. Iarriccio, J. Cassidy, M.S. Shet, R. Mannion, E. Donnell, A. Park, *Pharm. Res.* 2006, **23**, 1888 – 1897.

(25) N. Variankaval, R. Wenslow, J. Murry, R. Hartman, R. Helmy, E. Kwong, S.D. Clas, C. Dalton, I. Santos, *Cryst. Growth Des.* 2006, **6**, 690 – 700.

(26) *APEX2*, *SADABS and SAINT*; Bruker AXS inc, Madison, WI, USA, 2008.

(27) G. M. Sheldrick, *Acta Crystallogr.*, Sec A: Found. Crystallogr., 2008, **64**, 112.

(28) C. F. Macrae, I. J. Bruno, J. A. Chisholm, P. R. Edginton, P. McCabe, E. Pidocck, L. R. Monge, T. Taylor, J. Van de Streek, P. A. Wood, *J. Appl. Cryst.* 2008, **41**, 266.

(29) A. L. Spek, PLATON, Version 1.62, University of Utrecht, 1999.

(30) M. Neumann, *J Appl. Cryst.* 2003, **36**, 356 – 365.

(31) R.R. Seelam, S. Chandiran, K.R. Divi, K.N. Jayaveera, *Int. J. Pharm. Sci. Drug Res.* 2010, **2**, 188– 192.

(32) C.B. Hollabaugh, L.H. Burt, A.P. Walsh, *Ind. Eng. Chem.* 1945, **37**, 943 – 947.

(33) R. Kh, M. Khullarb, M. Kashyapb, P. Pandhi, R. Uppala, *J. Hypertens.* 2000, **18**, 919 – 926.

(34) G. Jagdeesh, Pharmacology reviews(s).
http://www.assessdata.fda.gov/....docs/.../20850_MICARDIS_pharmr_P1 (Assessed on 13-06-12)

(35) OECD, OECD guidelines for the testing of chemicals.2008.Test number 425. Acute oral toxicity– up-and-down-procedure (UDP).

(36) A.W. Newman, S.R. Byrn, *Drug DiscoveryToday*. 2003, **8**, 898 – 905
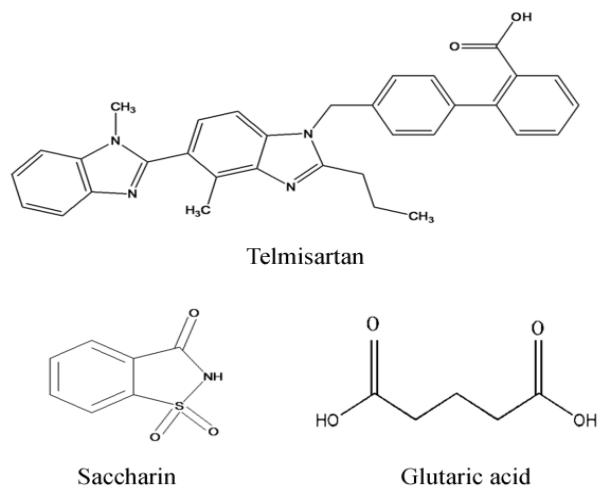
Scheme 1: Structures of Telmisartan, Saccharin and Glutaric acid.
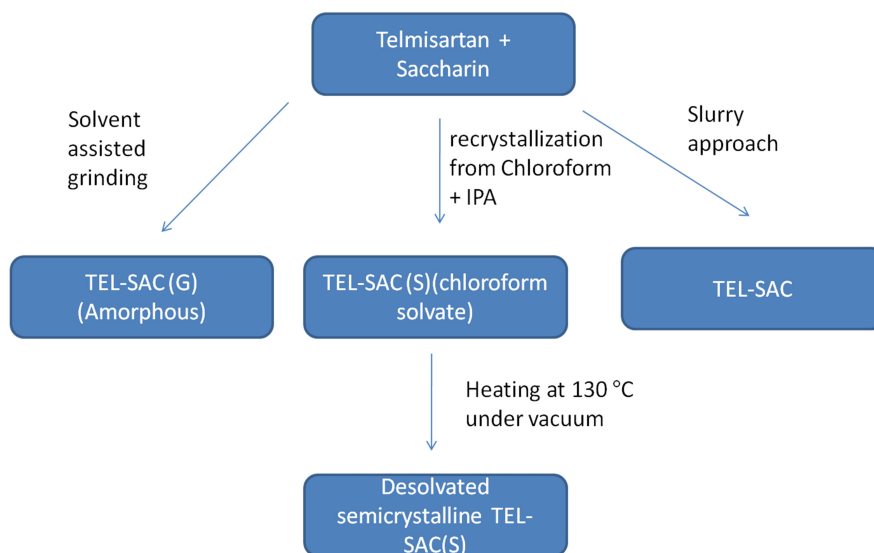
Scheme 2: Methods of cocrystallization of Telmisartan with saccharin
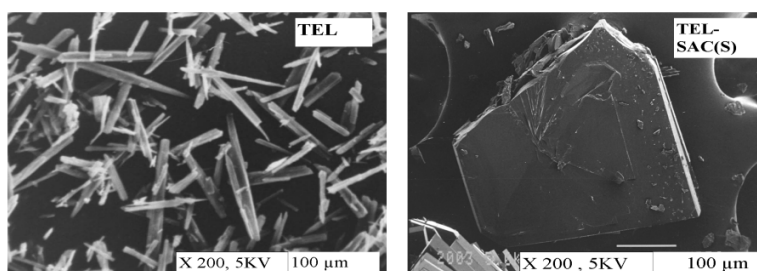
1

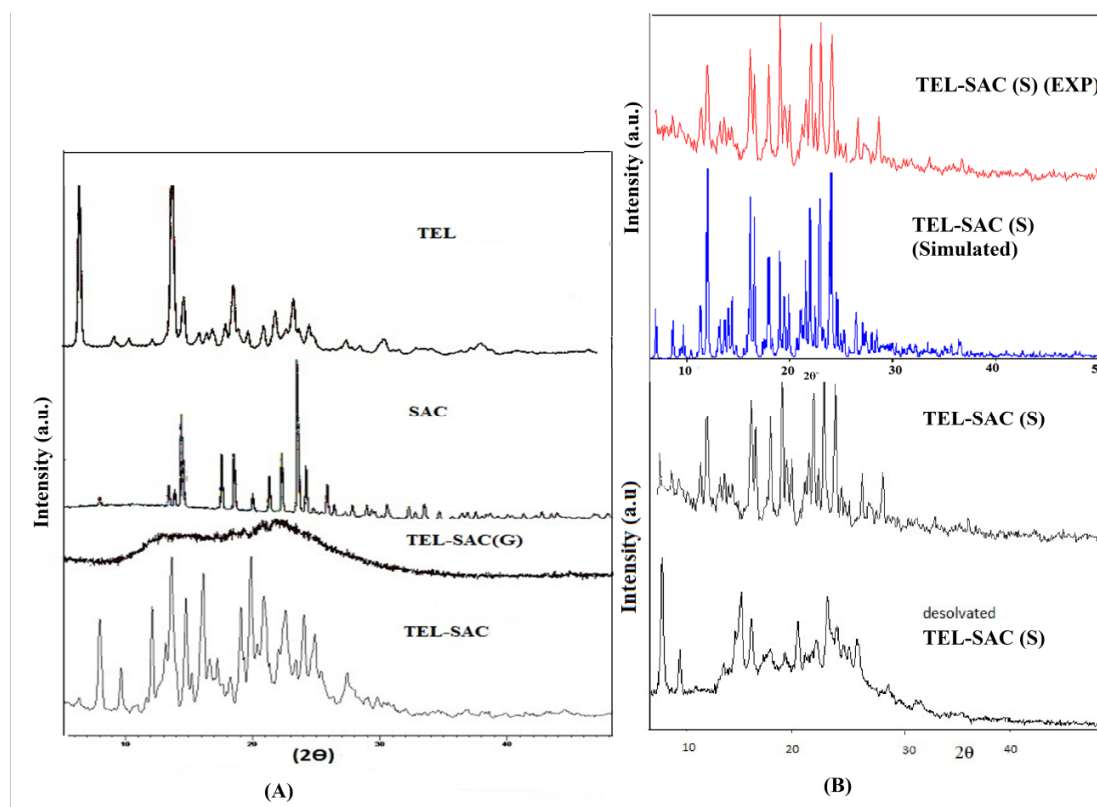Figure 1: SEM micrographs of TEL and TEL-SAC(S).

Figure 2 (A) PXRD patterns of TEL, SAC, TEL-SAC (G) and TEL-SAC; (B) Experimental PXRD (red) and simulated PXRD patterns of TEL- SAC(S) (blue) and PXRD patterns of TEL-SAC(S) and desolvated TEL-SAC(S).
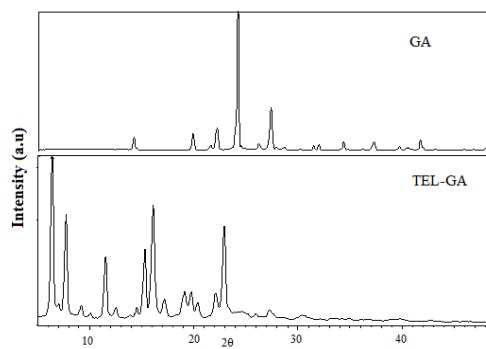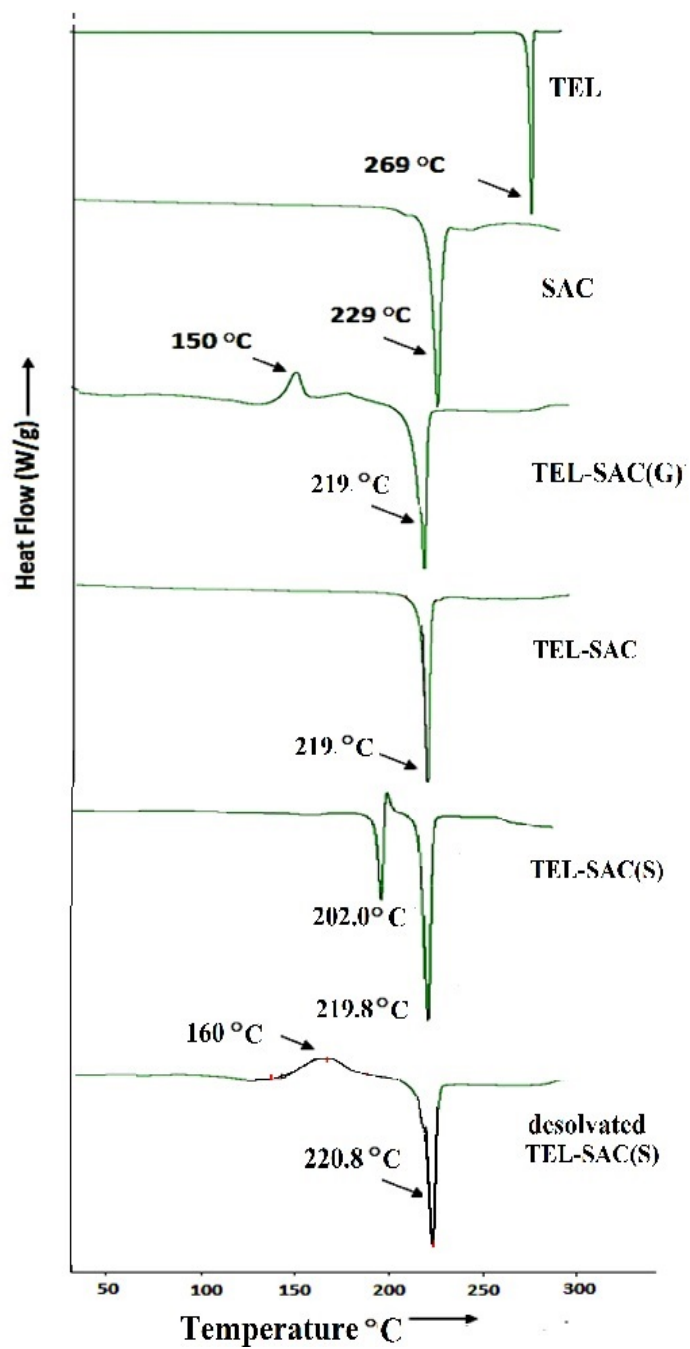
2

Figure 3: PXRD patterns of GA and TEL-GA.

Figure 4: DSC scans of TEL, SAC, TEL-SAC (G), TEL-SAC and TEL-SAC(S) and desolvated TEL-SAC(S).

4
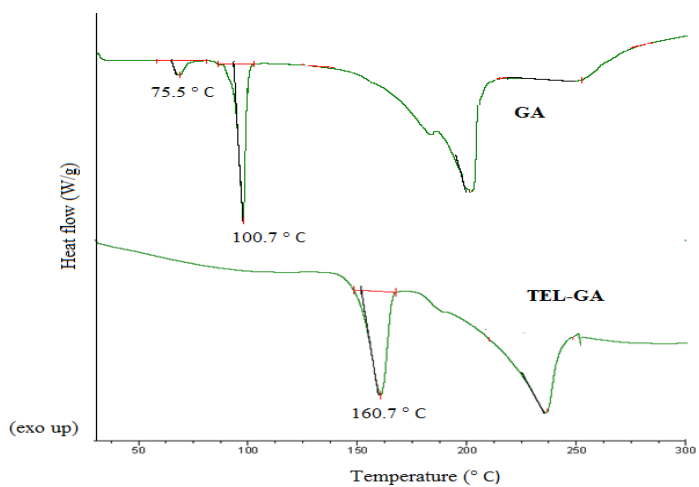
Figure 5A: DSC scans of GA and TEL-GA.
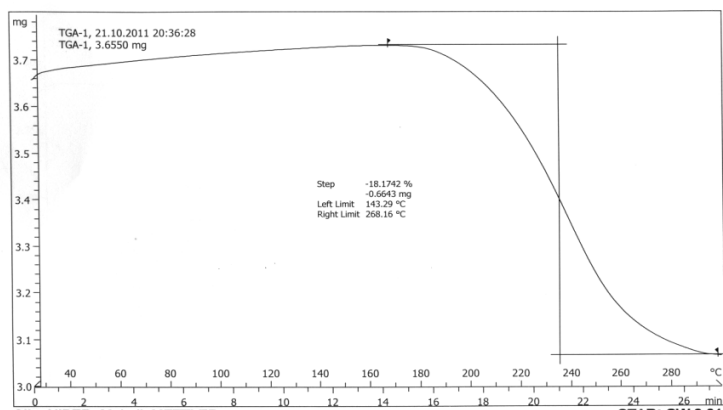
Figure 5B: TGA scan of TEL-GA.

5
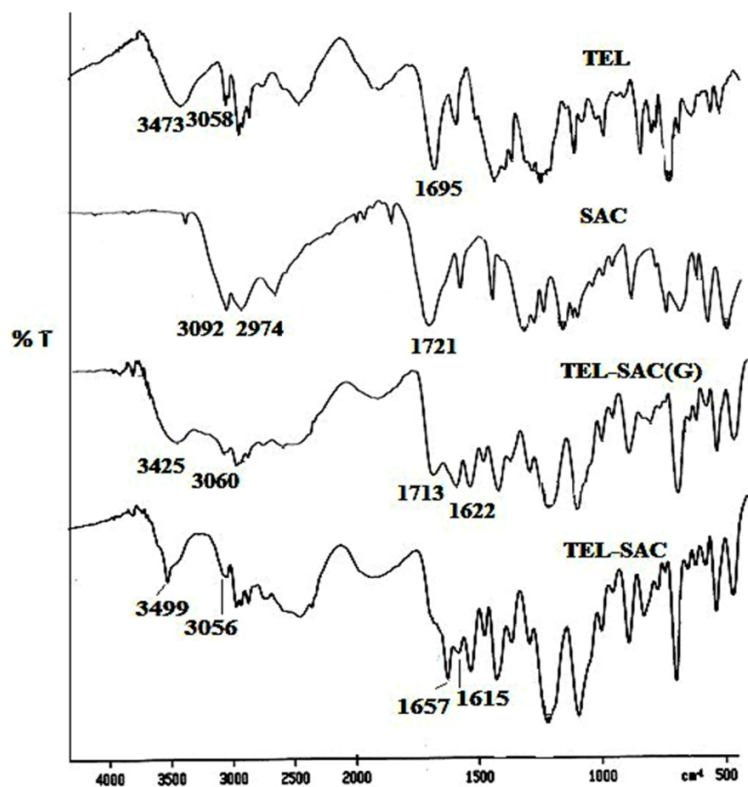
Figure 6A: FT-IR spectra of TEL, SAC, TEL-SAC (G) and TEL-SAC
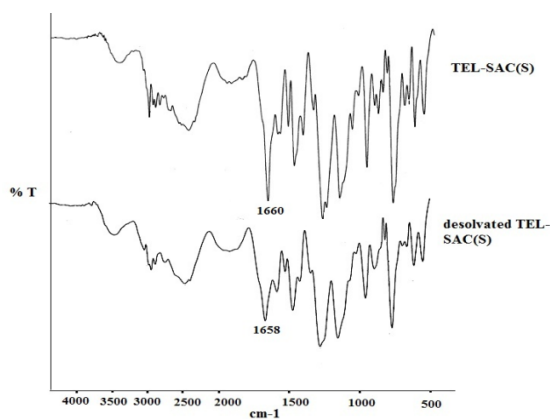
Figure 6B: FT-IR spectra of TEL-SAC(S) and desolvated TEL-SAC(S).

6
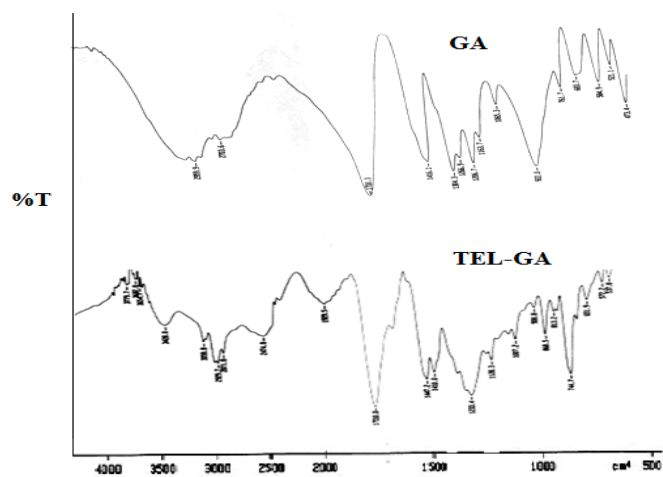
Figure 7: FT-IR spectra of GA and TEL-GA.
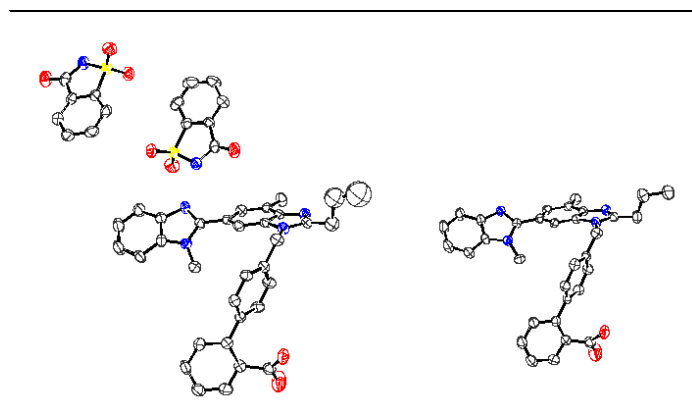
Figure 8: An ORTEP diagram of the TEL-SAC(S) cocrystal with 50% thermal ellipsoid probability. Solvent

molecules are not shown.

CrystEngComm Accepted Manuscript

7
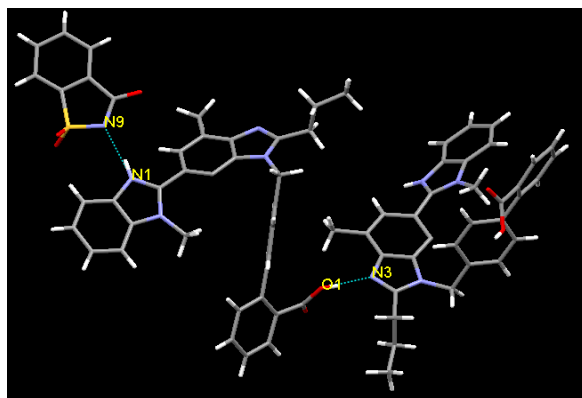
Figure 9A: Intermolecular H-bonding in TEL-SAC(S) (solvent molecules are not shown).
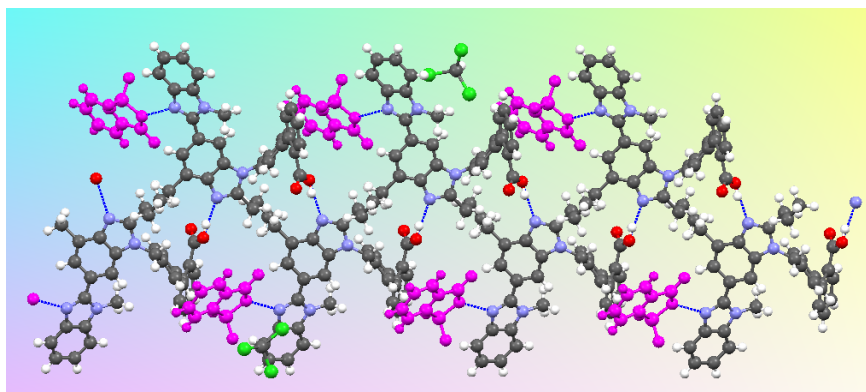
Figure 9B: Packing diagram of TEL-SAC(S) cocrystal; solvent molecules are present in the interstitial spaces.
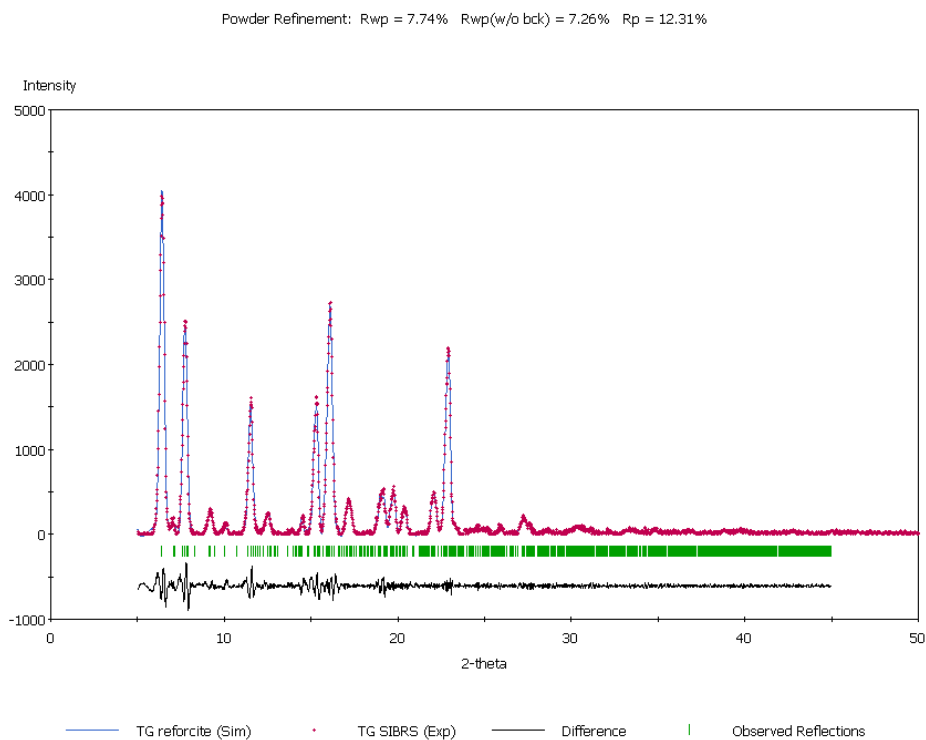
8

Figure 10: X-ray intensity in case of TEL-GA as a function of 2θ. Observed (experimental) pattern, calculated (best Rietveld fit profile) pattern, reflection positions and the difference curve between the observed and the calculated profile. (Rwp value = 7.74 %).
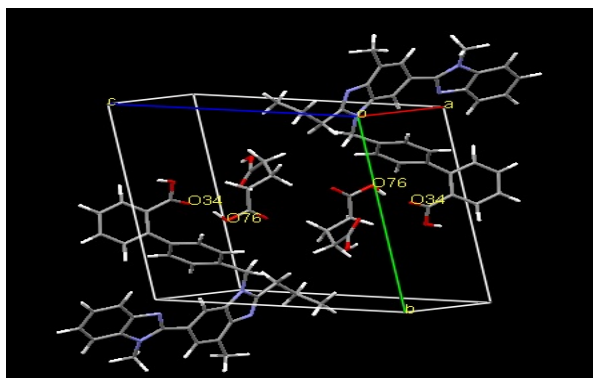
9

Figure 11 A: Arrangement of molecules in the unit cell in case of TEL-GA.
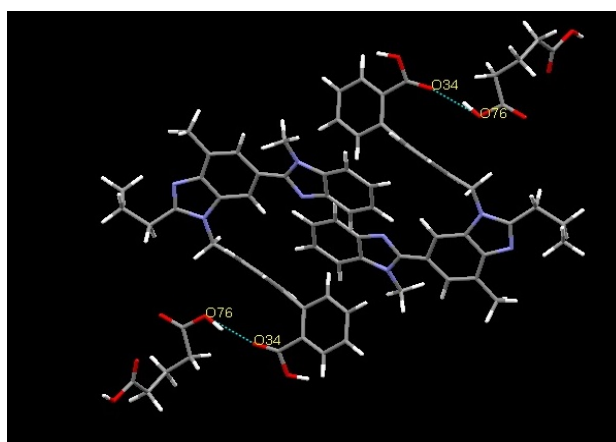

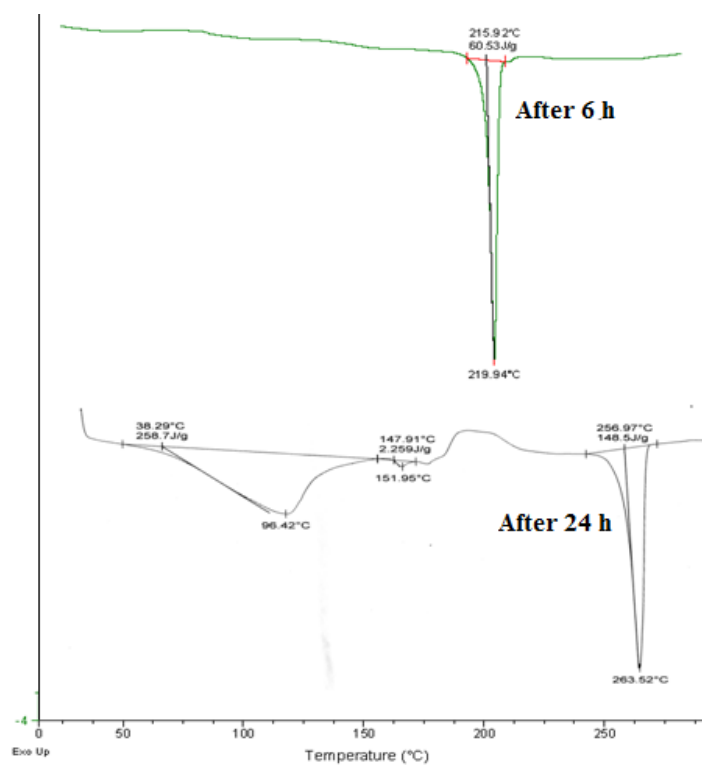Figure 11 B: H-bonding in TEL-GA co-crystal.

10

Figure 12: DSC scan of TEL-SAC after 6 hours and 24 hours of solubility.
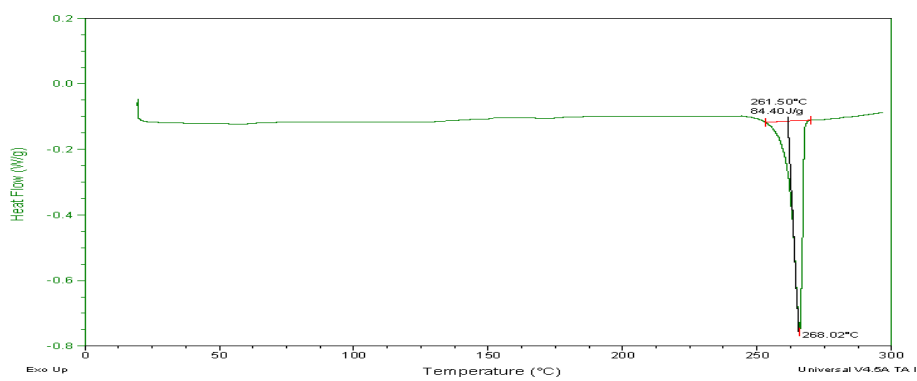

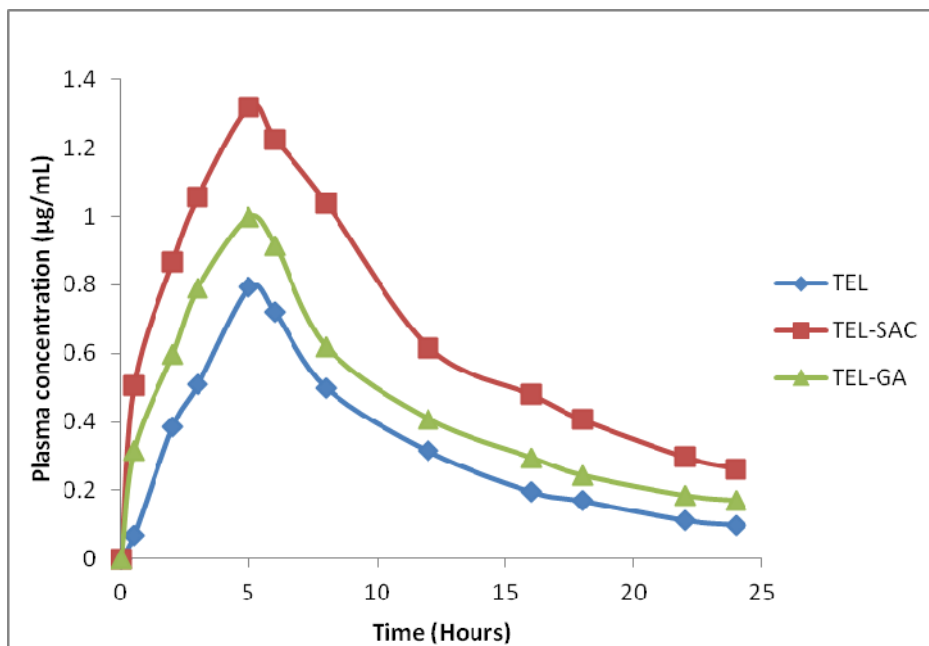Figure 13: DSC scan of TEL-GA after 6 hours of solubility.

11

Figure 14: Plasma concentration time profile after oral administration of TEL, TEL-SAC &TEL-GA
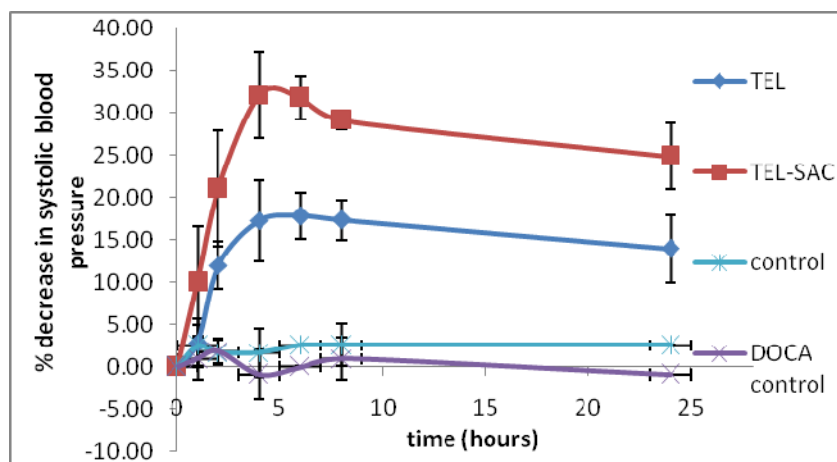

Figure 15: Antihypertensive activity of TEL-SAC in comparison to TEL (formA).
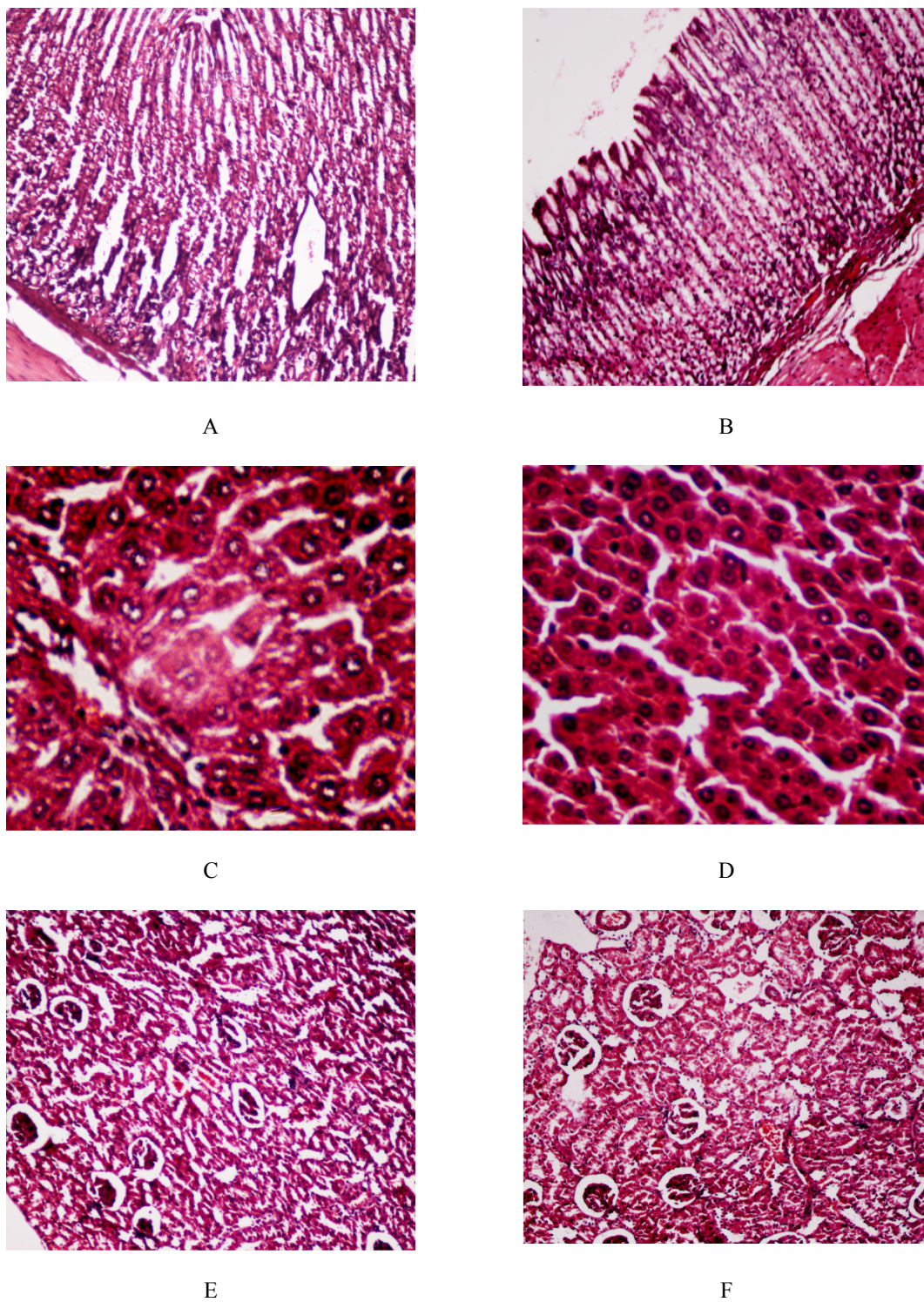
12

Figure 16: The microscopic pictures showing pathological changes at determined LD50 values (2000mg/Kg) of TEL and TEL-SAC

A) TEL: Stomach, B) TEL-SAC: Stomach, C) TEL: Liver, D) TEL-SAC: Liver, E) TEL: Kidney, F) TEL-SAC: Kidney.

13

Table 1: Crystallographic data for TEL-SAC(S)

Parameters	TEL-SAC(S)
chemical formula	$C_{41}H_{35}Cl_3N_5O_5S$
stoichiometry	1:1:1
formula wt	816.15
temperature (K)	200(2) K
wavelength (Å)	0.71073 Å
crystal system	monoclinic
space group	$P2_1/c$
a (Å)	37.8858(15)
b (Å)	13.3212(6)
c (Å)	15.7766(6)
α (deg)	90
β (deg)	101.541(2)
γ (deg)	90
Z	8
Cell vol (Å^3)	7801.2(6)
density (g·cm^{-3})	1.390
μ (mm^{-1})	0.340
F(000)	3384
θ (deg) range for data collection	2.02 to 25.10
reflns collected	56329
independent reflns	13831
reflns with I >2σ(I))	5337
R_{int}	0.1131
no. of parameters refined	984

14

GOF on F^2	0.846
final R_1^a/wR_2^b (I >2σ(I))	R_1 = 0.0630, wR_2 = 0.1372
weighted R_1/wR_2 (all data)	R_1 = 0.1780, wR_2 = 0.1738
largest diff. peak and hole (e·Å^{-3})	0.964 and -0.817 eÅ^{-3}
$^aR_1 = \Sigma\|\|F_o\| - \|F_c\|\|/\Sigma\|F_o\|$. $^bwR_2 = [\Sigma w(F_o^2 - F_c^2)^2/\Sigma w(F_o^2)^2]^{1/2}$, where $w = 1/[\sigma2(F_o^2) + (aP)^2 + bP]$, $P = (F_o^2 + 2F_c^2)/3$.	

Table 2: H-bond geometries of TEL-SAC(S)

Donor --- H....Acceptor	Symmetry	D - H (Å)	H...A (Å)	D...A (Å)	∠D-H...A
O(1) --H(1) ..N(3)	-x,-1/2+y,1/2-z	0.84	1.81	2.6463	171
O(3) --H(3A) ..N(7)	1-x,1/2+y,1/2-z	0.84	1.84	2.661	167
N(1) --H(6) ..N(9)		0.88	1.98	2.8505	169
C(2) --H(2) ..O(5)	x,1/2-y,-1/2+z	0.95	2.33	3.2763	179
C(5) --H(5) ..O(6)		0.95	2.43	3.3187	155
C(8) --H(8C) ..O(2)	-x,-y,-z	0.98	2.31	3.158	144
C(19) --H(19C) ..O(1)	x,-1/2-y,1/2+z	0.98	2.6	3.4889	151
C(23) --H(23) ..O(7)	x,-1+y,z	0.95	2.6	3.4185	145
C(35) --H(35) ..O(8)	x,3/2-y,1/2+z	0.95	2.41	3.3214	162
C(38) --H(38) ..O(10)	x,-1+y,z	0.95	2.49	3.33	148
C(41) --H(41A) ..O(4)	1-x,1-y,1-z	0.98	2.3	3.2178	155
C(41) --H(41C) ..O(8)	x,3/2-y,1/2+z	0.98	2.54	3.2794	133
C(58) --H(58) ..O(9)		0.95	2.54	3.16	123
C(79) --H(79) ..O(6)		0.95	2.57	3.3111	135
C(81) --H(81) ..O(10)	x,-1+y,z	1	2.16	3.1168	160
C(82) --H(82) ..O(6)		1	2.17	3.1026	154

15

Table 3: Crystallographic parameters of TEL-GA

Parameters	TEL-GA
Chemical formula	$C_{33}H_{30}N_4O_2 \cdot C_5H_8O_4$
Stoichiometry	1:1
Formula weight	646.7
Temperature (K)	Room temperature
crystal system	triclinic
space group	P-1
a (Å)	22.3598
b (Å)	15.6073
c (Å)	13.5310
α (deg)	94.4738
β (deg)	97.8221
γ (deg)	93.6366
vol (Å^3)	4650.68
2 θ range	4 °-45°

16

Table 4: Solubility of telmisartan and cocrystals (TEL-SAC & TEL-GA) in phosphate buffer pH 7.5 at 25 ºC (n=3)

Drug/Cocrystal	Solubility (μg/ml)
TEL	7.23 ± 0.321
TEL-SAC	14.40 ± 0.400
TEL-GA	63.23 ± 0.252

Table 5: Relative Pharmacokinetic parameters of telmisartan and cocrystal

Drug/cocrystal	Cmax (ng/mL)[a]	AUC_{0-t} (ng .h/mL) [b]	Rel. BA % [c]
TEL-SAC	1.318	16.38	2.07
TEL-GA	0.998	10.96	1.39
TEL	0.794	7.88	--

[a]Peak of maximum concentration.

[b]Area under the concentration time profile curve until last observation (upto 24 hours).

[c]Relative bioavailability of developed cocrystals with reference to pure drug.

17

Table 6: Changes in body weight before and after treatment

Treatment group	LD50 (mg/Kg BW)	Body Weight (Day 0)- in gram	Body weight (day 14)- in gram	Calculated t value at determined LD50	Remarks (S/NS)
TEL	2000	103± 4	108± 3	-1.732	NS*
TEL-SAC	2000	107± 6	114± 4	-1.681	NS**

S-Significant ; NS-Not significant; * Power of performed test with alpha = 0.010: 0.051, ** Power of performed test with alpha = 0.010: 0.047

Table 7: Body weight of individual animals (as required by OECD TG 425) at all tested doses on day 7 and day 14 after administration of single oral doses in ascending order.

Treatment group	Dose group (mg/Kg BW)	Animal code	Body Weight (Day0) in gram	Body weight (day7) in gram	Body weight (day 14) in gram
TEL	175	TEL-1	110	112	118
	550	TEL-2	110	114	120
	2000	TEL-3	100	100	106
	2000	TEL-4	102	106	106
	2000	TEL-5	108	110	112
TEL-SAC	175	TEL-SAC-1	110	116	122
	550	TEL-SAC-2	120	128	130
	2000	TEL-SAC-3	100	106	110
	2000	TEL-SAC-4	110	114	118
	2000	TEL-SAC-5	110	110	114

18